

Experimental Testing System for Adsorption Space Heating

Urška Mlakar^{1*} – Rok Koželj¹ – Alenka Ristić² – Uroš Stritih¹

¹ University of Ljubljana, Faculty of Mechanical Engineering, Slovenia

² National Institute of Chemistry, Slovenia

Approximately 40 % of the final energy is used for heating and cooling of buildings. Of this, as much as 75 % is used in residential buildings. The proportion of energy needed in buildings is relatively high, so it is necessary to start using technologies that have low energy consumption, use it efficiently or provide it from renewable sources. One such technology is thermal energy storage, which allows us to store excess energy for later when we need extra energy. The paper presents two experiments in the field of adsorption space heating. In the first experiment, measurements were carried out on the adsorbents - zeolite 13X and zeolite NaYBFK, which were placed into a duct, through which humid air was transported by means of a centrifugal fan. In the second experiment, water vapour as the working medium was used. With the first experiment we achieved better water uptake on NaYBF, while the second experiment shows the increase of water uptake of zeolite 13X.

Keywords: sorption heat storage, space heating, water vapour, humid air, zeolite 13X, zeolite NaYBFK

Highlights

- Zeolite NaYBFK achieves lower maximum temperature, but has better water uptake than zeolite 13X, when humid air is used as the working fluid.
- Water uptake of zeolite 13X can be improved with higher inlet temperature of water vapour, while reached maximum temperature during adsorption phase is lower.
- The maximum temperature during adsorption increased for 24 °C for zeolite NaYBFK with water vapour and the water uptake did not change at the same inlet temperature.
- A lower inlet temperature and a smaller amount of NaYBFK reaches a higher maximum temperature, while the heat of adsorption phase lasts longer, when water vapour was used.

0 INTRODUCTION

If we want to improve the efficiency of systems in the building sector in future generations, the application of storage technologies will be necessary. Storage technologies allow us to store energy during times of excess energy and use it when needs are greater. Energy can be stored in sensible, latent [1], and thermochemical storage technologies (absorption and adsorption) [2]. Such technologies can be applied in both heating and cooling, for different storage periods. The example we discussed in this paper is suitable for building space heating applications.

Based on a review of the literature, it was found that zeolite 13X is used in research of several thermal energy storage (TES) systems. Stritih and Mlakar [3] presented sorption systems, important characteristics of the materials used and some open and closed systems in a chapter, which also include few examples where zeolite 13X was used. It was used in the research by Dawoud and Amer [4], who considered a closed TES system with a working pair of 13X - water. Tatsidjodoung et al. [5] investigated the case of an open system with 13X zeolite and water, the system was intended for use in buildings and obtained energy for storage from solar energy. We also found a case where a working pair of zeolite 13X-water is

being tested in industry, as discussed by Schreiber et al. [6] in their research. Zeolite 13X is also used in another combination of working mediums, such as 13X-magnesium sulfate and water, as investigated by Xu et al. [7].

The above research shows that zeolite 13X is suitable for use in building systems. Compared to silica gel, 13X zeolite can provide higher temperature lifts [8]. For binderless zeolite 13X beads the water adsorption isotherms and the adsorption kinetics have been studied in detail by experimental investigation in a sorption analyzer (adsorption isotherms) and fixed bed reactor (adsorption kinetics) by Mette et al. [9]. Experimental investigations have shown that this zeolite is characterized by a high-water uptake and fast reaction kinetics. Both properties are of great importance when using this material for thermochemical energy storage application. A high-water uptake is required for a high energy storage density whereas high sorption kinetics is essential for a high thermal power output during adsorption. Banaei and Zanji [10] focused on different utilization of zeolite 13X and main challenges such as compact system design, charging supply, humidity management, system output power, and system efficiency. Rogala et al. [11] proposed a novel model useful for analyzing the silica gel-water adsorption

*Corr. Author's Address: University of Ljubljana, Faculty of Mechanical Engineering, Slovenia, urska.mlakar@fs.uni-lj.si

1 ADSORPTION HEATING

and desorption process in air-fluidized systems. Presented model is especially reliable tool for silica gel particle diameters from 1 mm to 3 mm. Model was validated through an extensive experimental study, which was carried out on the laboratory test-stand. Antonellis et al. [12] studied open sorption thermal energy storage system based on zeolite 13X and its integration at system level through an experimental and a numerical approach. The study provides a methodology for determining the efficiency of a complete thermal storage system with an adsorption TES as well as identifying possible engineering applications of such a technology. Through literature review could be observed that zeolite 13X is the most widely researched and obtainable sorption material, that's also why it was used in our comparison with other zeolite material.

In our work we focused on zeolite 13X, which is presented in the literature as a promising medium for sorption energy storage in building systems. At the same time, we wanted to compare the already known zeolite 13X with another sorption material - zeolite NaYBFK.

The paper discusses energy storage in the summer for the purpose of the use in the winter - technology of seasonal storage. With the applications of such technologies, energy can be used more efficiently. Our system is an open adsorption system that uses air to which water vapour is added (e.g. humid air) and water vapor, as working media. The temperature of these working media allows the activation of the adsorbent material to initiate heat release. The heat released during the adsorption phase can then be used as a heating source. The aim of the research was to obtain experimental data for the adsorption phase for zeolite 13X (Silkem, Slovenia) and zeolite NaYBFK (CWK, Germany), which would later be used to verify the results obtained by simulation in the Ansys environment. In the analysis of the results, we focused on the maximum achieved temperature in the adsorption phase, the duration of adsorption phase and the achieved water uptake.

This paper consists of 4 chapters. Chapter 1 presents adsorption heating in all three stages of the process, using a p-T-x diagram. Chapter 2 presents the performed experiments together with their measuring setup and the equipment used. Chapter 3 first presents an explanation of the temperatures measured in the experiments, and then presents the results of each experiment in two subchapters. The paper concludes with a final discussion.

The circular process in adsorption storage is the same as the circular process of a heat pump, the difference is only in the interruption of operation between the processes of desorption and adsorption. This interruption represents a time when stored energy is not needed. Fig. 1 shows a p-T-x diagram of an adsorption heat storage process.

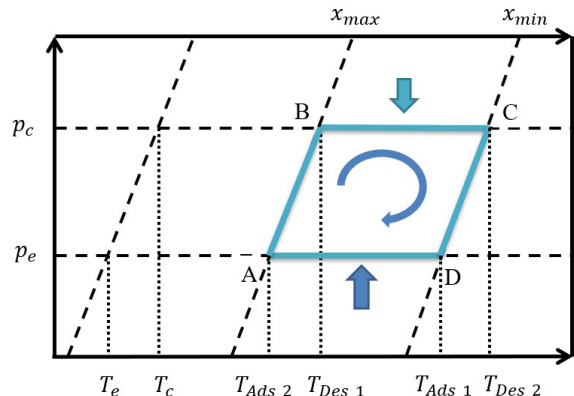


Fig. 1. p-T-x diagram of an adsorption heat storage process

The mass of the adsorbate varies between the minimum (line C, D) and the maximum value (line A, B). The adsorption process takes place between points D-A at the evaporation pressure p_e and desorption process takes place at pressure p_c between points B-C. This work cycle consists of the following four steps:

Step 1: The storage of heat in the bulk region - adsorber begins with isosteric (humidity is constant) heating of the adsorbent. The pressure and temperature in the adsorber increase in line from point A to point B until the initial desorption temperature T_{Des_1} is reached. At this temperature, the pressure in the adsorber equals the condensation pressure of the adsorbed working medium (at point B).

Step 2: At point B, the desorption phase will start. The adsorbent is heated until working medium is removed, and the adsorbent becomes dry (the lines between points B and C). This is when the maximum available temperature T_{Des_2} is reached. Meanwhile, the condenser is cooled to maintain the condensation pressure p_c . The heat generated by condensation (Q_c) is discharged to the surroundings as waste heat. This affects the condensation temperature T_c , which must be kept as low as possible to ensure the best desorption possible. At the maximum reached temperature T_{Des_2} , the degree of saturation of the adsorbent with the adsorbate is minimum x_{min} , so the cycle is completed.

Step 3: Depending on the time period of energy storage and ambient temperature, the temperature in the storage region may fall during this period. The drop in temperature and, consequently, the pressure, shows an isostere between C and D. The temperature may decrease to the initial adsorption temperature T_{Ads_1} or even lower.

Step 4: Emptying the stored heat begins by supplying heat to the adsorber. We can supply heat from various sources (solar collectors, earth heat). The working medium is evaporated at the evaporation pressure p_e and the temperature T_e . Currently the working medium is adsorbed on the adsorbent and heat is released - Q_{Ads} (the line between points D and A). The released heat is called usable heat that can be used in the heating system.

This paper presents the adsorption phase of the storage process which can be used for heating of the building in the winter.

2 EXPERIMENTAL

Two experiments were conducted on the adsorption process of working fluid on the bulk using the zeolite 13X and zeolite NaYBFK. In the first experiment, the

working medium was humid air, e.g. air to which water vapour was added from ultrasonic humidifier, while in the second experiment, water vapour was used as the working medium. Temperatures measurements of adsorption process were performed to validate the numerical model. Fig. 2 shows the scheme of the experimental setup for sorption process.

The system has two key parts of the experimental line, namely the centrifugal fan (1) and the compartment with the adsorption substance bulk. By adjusting the frequency on the frequency regulator (2), the speed of the centrifugal fan that drives air through the duct is controlled. Air velocity into the duct was measured using a vane anemometer (3). After vane anemometer the first thermocouple (4) was positioned to measure temperature of the air in the duct. The vane anemometer, the first thermocouple, hygrometer and the pressure transmitter are connected to the TESTO 400 data logger (5), where the measurement data is collected. A pressure converter (6) was also used to convert the pressure before entering the porous bed and the pressure after the porous bed. The pressure difference meter thus measures a pressure drop through the packed bed of the adsorption material. We also carried out an indirect measurement of air flow

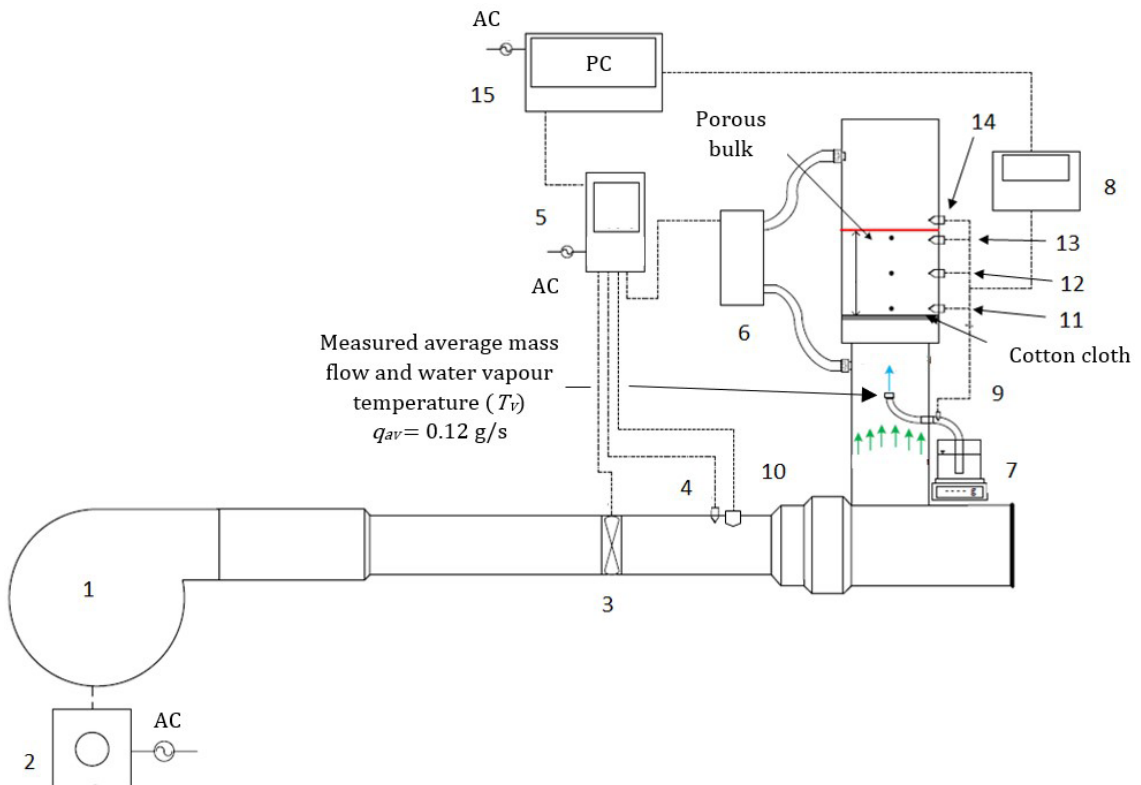


Fig. 2. Experimental setup for adsorption space heating system

through the duct as shown with green arrows. Water vapour was added to the working medium - air, thus moistening it. The mass flow of water vapour that was added to the air was determined with difference in weight of water in ultrasonic humidifier (7) and time measurement. The water vapour temperature measurement data and the porous temperature data measured with thermocouples were linked to Agilent 34970a data logger (8). In addition to the flow that is shown as blue arrow on the experimental setup, we also measured the water vapour temperature (9) that was added to the air flow. After vane anemometer and the first thermocouple, hygrometer (10) was positioned to measure humidity of the air in the duct. When water vapour was added to the air, these two streams were mixed before entering the porous bulk. In the porous bulk the temperatures were measured at different locations or heights. The first temperature (11) was measured immediately behind the cotton fabric at the bottom of the porous bulk. The second temperature (12) was measured at medium height of the porous bulk. The next thermocouple (13) was located at the top of the porous packed bed. The last thermocouple (14) measured the air temperature behind the porous packed bed. The measurements of all the meters were collected on a computer (15).



Fig. 3. Adsorber with bulk of zeolite 13X

The boundary conditions of the first experiment were as follows: The volume of the porous packed bed was 281 ml (zeolite 13X), 260 ml, 280 ml and 180 ml (zeolite NaYBfK), and the mass of the porous material was 173 g, 192 g, 200 g and 134 g, respectively. The height of the porous bulk was 25.7 mm. The mass flow of water vapour varied in the range from 0.05 to 0.1 g/s. Time interval of measurement reading was 10 seconds. The Zeolite 13X porous bulk (Fig. 3) had a granulation size between 1.6 mm and 2.5 mm.

The experimental setup for the second experiment is part of the experimental setup of the first experiment. The difference is that this time we

only use water vapour as a working medium. By supplying water vapour as working medium, we got rid of the problem of efficient mixing of air and water vapour before entering a porous bulk. As in the first experiment, this time we measured the water vapour temperature, the water vapour mass flow, and the temperatures in the porous bulk at different heights. The flow of water vapour is shown in the Fig. 4 with a blue arrow.

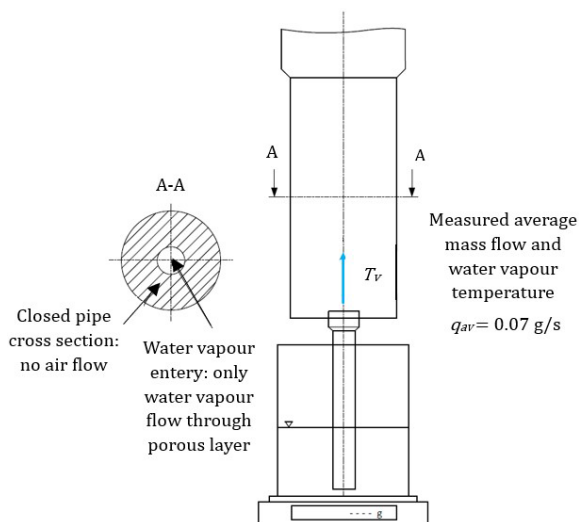


Fig. 4. Experimental setup for experiment with water vapour as working medium

Experimental setup is shown in Fig. 5.

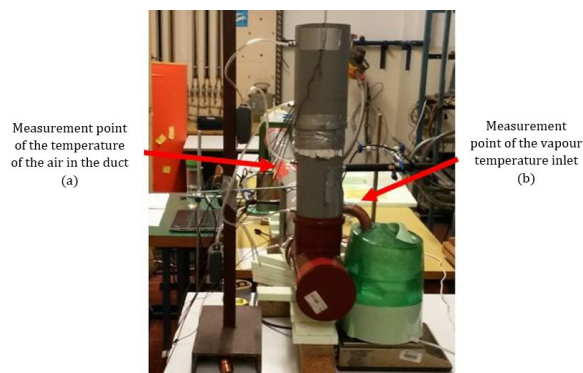


Fig. 5. Measurement points of water vapour temperature inlet and temperature of the air in the duct

3 RESULTS

In the following sections, the temperature measurements of each set of experiments are shown in graphs. The results show 7 different temperatures:

- Duct temperature (a) is the temperature of the air in the horizontal duct in the first experimental

setup as shown in the Fig. 2 (measured at number 4).

- Temperature (b) is the temperature of a water vapour inlet in the first and second experiment
- Temperature (c) is the temperature that was measured at the bottom of the packed bed on 1/4 of the cross section of the duct.
- Temperature (d) is the temperature that was measured at the bottom of the zeolite bulk in the middle of the cross section of the duct.
- Temperature (e) is the temperature that was measured at the bottom of the zeolite bulk on 3/4 of the cross section of the duct.
- Temperature (f) is the temperature that was measured at the bottom edge of the zeolite bulk.
- Temperature (g) is the temperature that was measured at the top of the zeolite bulk on 1/4 of the cross section of the duct. On the experimental line in Fig. 2 the thermocouple for measuring this temperature is marked with the number 12.

Fig. 5 shows the measuring point of the temperature of the water vapour entering the duct and the air temperature in the horizontal duct.

Figs. 6 and 7 shows the thermocouples used to measure the temperatures in the zeolite bulk in the adsorber.



Fig. 6. Measurement points of the temperatures that were measured at the bottom of zeolite bulk

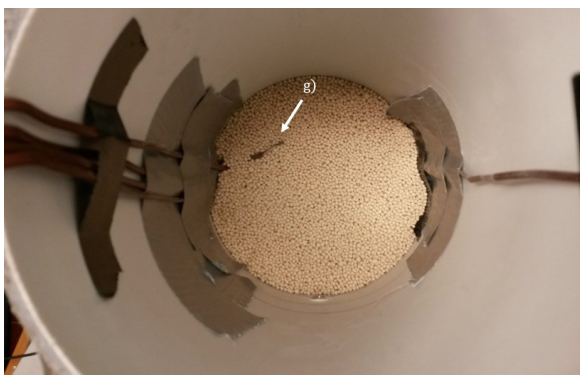


Fig. 7. Thermocouple (g) at the top of the zeolite bulk

Several sets of measurements were performed for each experiment. For the first experiment, we performed three sets of measurements: one for zeolite 13X and two for zeolite NaYBfK.

For the second experiment, we performed two sets of measurements:

- one for zeolite 13X,
- one for zeolite NaYBfK.

4.1 First Experiment

The results of the first experiment are shown in the following figures. In the first set of measurements, conditions were as follows: The used adsorbent was zeolite 13X with the amount of 173 g. The average water vapour inlet temperature was 22 °C in the interval from 20 to 91 (time span of 12 minutes). The maximum temperature reached was 128 °C. The water uptake of 0.22 kg_w/kg_a was reached. Fig. 8 shows the measured temperatures in the packed bed at different locations.

In addition to temperatures, Fig. 9 also shows the air velocity through the bulk. We had a water vapour inflow from interval of 20 to 91, with a very slow velocity - performing adsorption. When the water vapour supply stopped at interval 91, the air velocity was increased to remove heat from the adsorbent by blowing air. It can be observed that at interval 91, the air velocity suddenly increases to 0.9 m/s, and consequently a decrease in temperatures occurs. The adsorption phase is completed. Forced heat dissipation occurs, which takes about 16 minutes. Temperatures drop to around 25 °C.

The results of the first measurements for zeolite NaYBfK are shown in the following figures. In the first set of measurement, conditions for zeolite NaYBfK were as follows: The amount was 192 g. The average water vapour inlet temperature was 22 °C in the interval from 73 to 204 (time span of 22 minutes). The maximum temperature reached was 110 °C, the water uptake for zeolite NaYBfK was determined to be 0.25 kg_w/kg_a. Fig. 10 shows temperatures in the zeolite packed bed at different heights.

At interval 180 the air velocity suddenly increases to remove heat from the adsorbent and consequently a decrease in temperatures occurs after the adsorption phase is completed. Temperatures drop to around 25 °C in about 8 minutes after the forced dissipation occurs.

In the second set of measurement conditions for the zeolite NaYBfK were as follows: The quantity of the zeolite was 200 g. The average water vapour

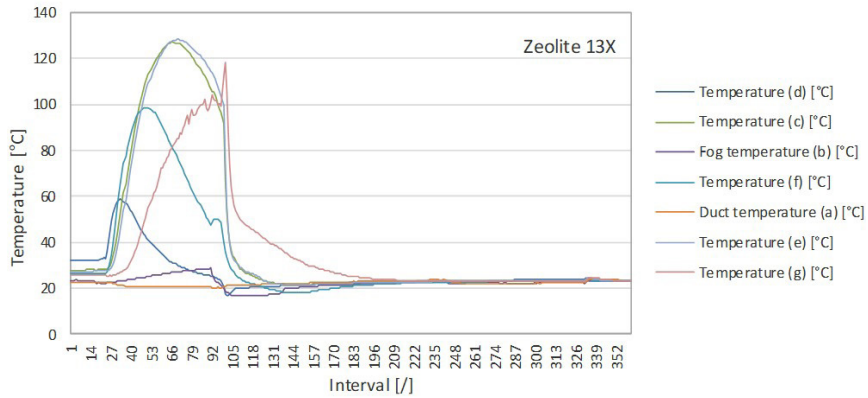


Fig. 8. Temperatures in packed bed of zeolite 13X during the first set of conditions

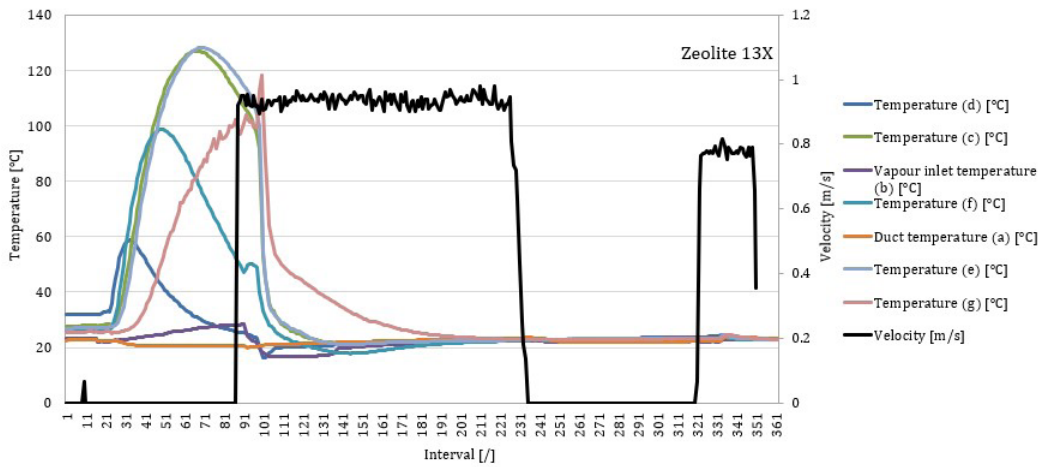


Fig. 9. Temperatures in zeolite 13X bulk and air velocity during the first set of conditions

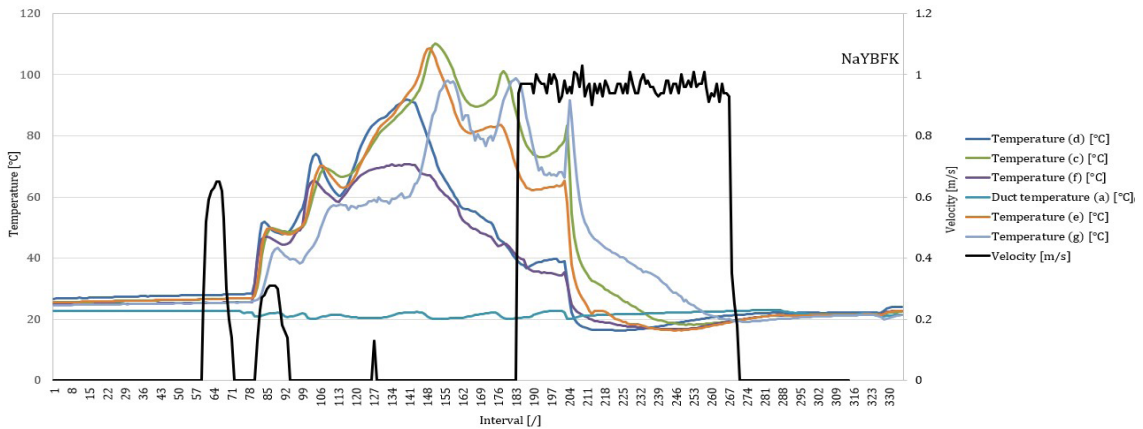


Fig. 10. Temperatures in the zeolite NaYBFK bulk during the first set of conditions for NaYBFK

inlet temperature was 22 °C in the interval from 23 to 178 (time span of 26 minutes). The maximum temperature reached was 97 °C. The water uptake of zeolite NaYBFK was 0.26 kg_w/kg_a. Fig. 11 shows temperatures in the packed bed at different heights and air velocity

At interval 178 the air velocity suddenly increases to remove heat from the adsorbent and consequently a decrease in temperatures occurs, after the adsorption phase is completed. Temperatures drop to around 25 °C in about 6 minutes after the forced dissipation occurs.

The inflection of temperature curve is due to the return flow, where inlet of water vapour does not flow through packed bed. When the steadiness of the flow of water vapour and air in the system is restored, the adsorption process in the porous layer starts again. Therefore, the inflection point is due to unsteadiness of the flow of water vapour in the system.

4.2 Second Experiment

Results of measurements of the second experiment are presented below. The difference is that water vapour as a working medium has been used.

The boundary conditions of the last experiment with zeolite 13X were as follows: The volume of the bulk was 281 ml, and the amount was 173 grams. The height of the bulk was 25.7 mm. The mass flow of water vapour was 0.12 g/s. The zeolite 13X bulk had a size of granules between 1.6 mm and 2.5 mm. The average water vapour inlet temperature was 28 °C in the interval from 34 to 228 (time span of 32 minutes). The maximum reached temperature was 120 °C and the water uptake of material was 0.27 kg_w/kg_a.

Fig. 12 shows temperatures at different layers of the porous packed bed in the period before the start of the adsorption phase, during the adsorption

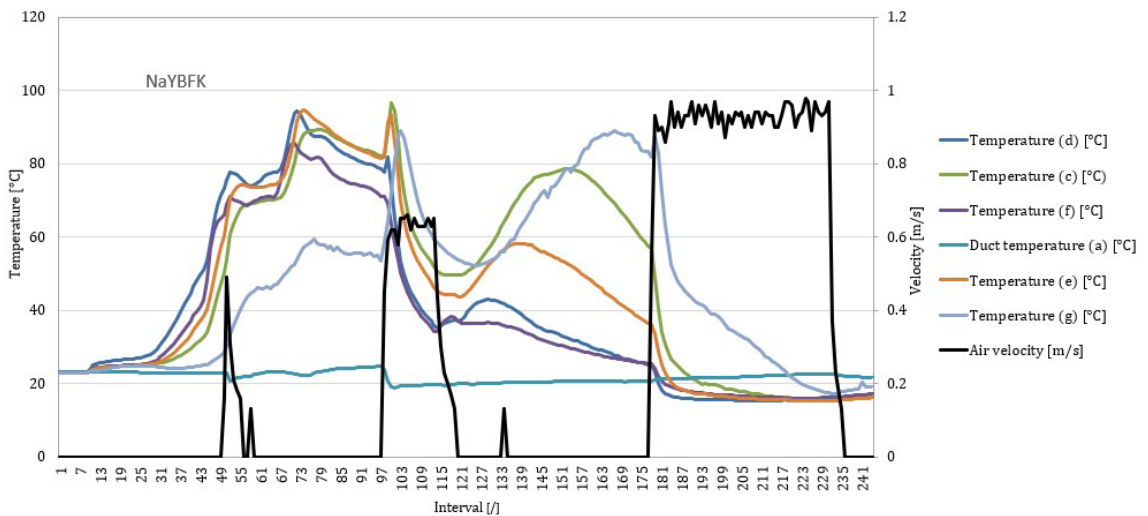


Fig. 11. Temperatures in the zeolite NaYBFK packed bed and air velocity during the second set of conditions

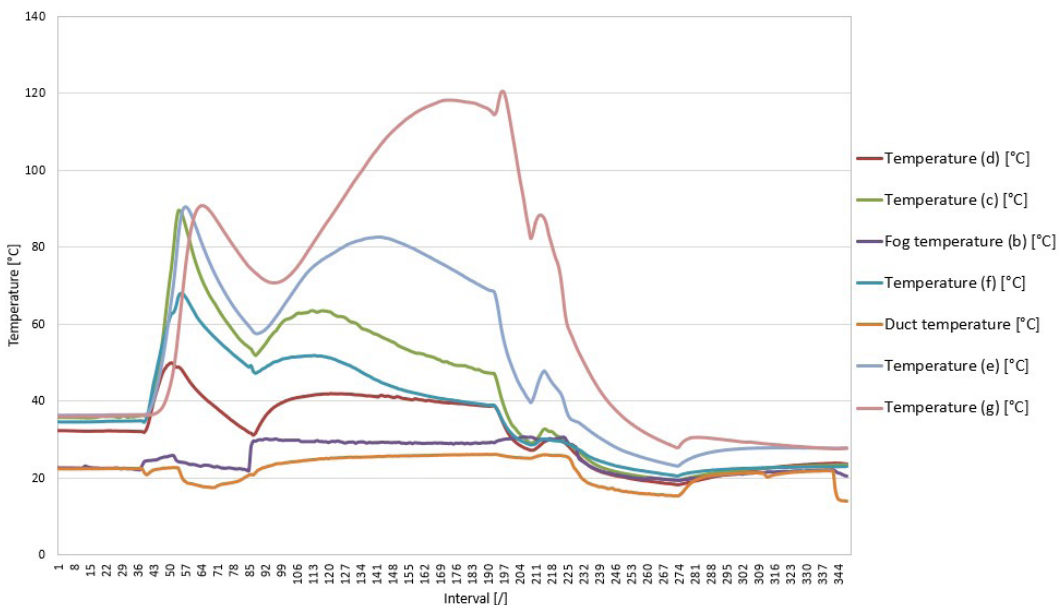


Fig. 12. Temperatures in bulk during the second set of conditions for zeolite 13X

phase and after the adsorption phase was completed. Two infection points of temperature distribution can be seen from Fig. 12. This is the consequence of desorption of the packed bed layers that already went through adsorption process. The layers that are going through the adsorption process are emitting heat to the adjacent layers that already went through the adsorption and are now desorbing.

The results of the measurements for zeolite NaYBFK are shown in Fig. 13. At this experiment, measurement conditions for zeolite NaYBFK were as follows: the mass was 134 g. The average water vapour inlet temperature was 22 °C in the interval from 35 to 96 (time span of 10 minutes). The mass flow of steam was 0.07 g/s. The maximum temperature reached was 134 °C. The water uptake was 0.25 kg_w/kg_a.

At time interval of 35 intake of water vapour starts to flow through packed bed and the adsorption process starts. The water vapour flows through the packed bed up to the time interval of 96. After the adsorption process, the air is imposed to the system at time interval of 141 to cool down the material. The reached peak temperature is 130 °C. Temperatures drop to around 25 °C in about 23 minutes after the forced dissipation occurs.

5 CONCLUSIONS

Two experiments were conducted on the adsorption process on the bulks of zeolite 13X and zeolite NaYBFK as the adsorbents. From all the results it can be seen that the temperature distribution in the packed

bed changes depending on the cross-section of the packed bed (we have a lower maximum temperature at the edges). Comparing two measurements for zeolite NaYBFK for the first experiment, we see that a larger quantity (8 g more) of the sorption material achieves a maximum temperature that is 13 °C lower, but at the same time has slightly better water uptake.

A comparison of zeolite 13X and NaYBFK for the first experiment shows that zeolite NaYBFK reaches a lower maximum temperature but has better water uptake, and that released heat during adsorption phase lasts longer with zeolite 13X. A comparison of the first and second experiment for zeolite 13X shows that with the same amount of sorption material (173 g), but a few degrees higher inlet temperature of the mist in the second experiment (28 °C), a better water uptake is achieved (1st experiment 0.22 kg_w/kg_a, 2nd experiment 0.27 kg_w/kg_a), but at the same time the maximum temperature reached is 8 °C lower. Comparing the 1st and 2nd test for zeolite NaYBFK shows that the same water adsorption is achieved with a smaller amount of sorption material (58 g less) at the same inlet temperature, but at the same time the maximum temperature reached in the 2nd experiment is 8 °C lower. The results of the second experiment shows that zeolite NaYBFK reaches a higher maximum temperature (14 °C higher) at a lower inlet temperature than zeolite 13 X and a lower amount of the sorption material (39 g less), while the heat during adsorption phase lasts longer (11 minutes longer).

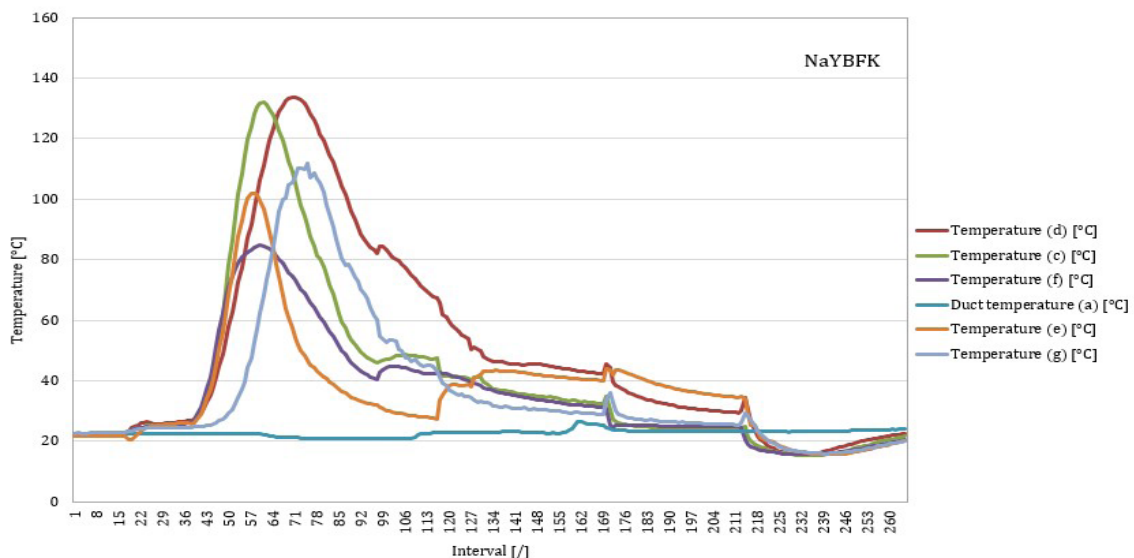


Fig. 13. Temperatures in packed bed during the set of conditions for zeolite NaYBFK with water vapour as working medium

6 ACKNOWLEDGEMENTS

This study was financially supported by Slovenian Research Innovation Agency (ARIS) through project number L1-7665.

7 REFERENCES

- [1] Kittusamy, R. K., Rajagopal, V., and Felix, P. G. (2022). Preparation and thermal characterization of nanographene-enhanced fatty acid-based solid-liquid organic phase change material composites for thermal energy storage. *Strojniški Vestnik - Journal of Mechanical Engineering*, vol. 68, no. 7-8, p. 461-470, DOI:10.5545/sv-jme.2022.148.
- [2] Wu, W. (2020). Low-temperature compression-assisted absorption thermal energy storage using ionic liquids. *Energy and Built Environment*, vol. 1, no. 2, p. 139-148, DOI:10.1016/j.enbenv.2019.11.001.
- [3] Stritih, U., Mlakar, U. (2018). Technologies for seasonal solar energy storage in buildings. *InTech*, p. 51-75, DOI:10.5772/intechopen.74404.
- [4] Dawoud, B., Amer, E.-H., Gross, D.-M. (2007). Experimental investigation of an adsorptive thermal energy storage. *International Journal of Energy Research*, vol. 31, no. 2, p. 135-147, DOI:10.1002/er.1235.
- [5] Tatsidjoudoung, P., Le Pierrès, N., Heintz, J., Lagre, D., Luo, L., Durier, F. (2016). Experimental and numerical investigations of a zeolite 13X/water reactor for solar heat storage in buildings. *Energy Conversion and Management*, vol. 108, p. 488-500, DOI:10.1016/j.enconman.2015.11.011.
- [6] Schreiber, H., Graf, S., Lanzerath, F., Bardow, A. (2015). Adsorption thermal energy storage for cogeneration in industrial batch processes: Experiment, dynamic modeling and system analysis. *Applied Thermal Engineering*, vol. 89, p. 485-493, DOI:10.1016/j.applthermaleng.2015.06.016.
- [7] Xu, S.Z., Lemington, Wang, R.Z., Wang, L.W., Zhu, J. (2018). A zeolite 13X/magnesium sulfate-water sorption thermal energy storage device for domestic heating. *Energy Conversion and Management*, vol. 171, p. 98-109, DOI:10.1016/j.enconman.2018.05.077.
- [8] Yu, N., Wang, R.Z., Wang, L.W. (2013). Sorption thermal storage for solar energy. *Progress in Energy and Combustion Science*, vol. 39, no. 5, p. 489-514, DOI:10.1016/j.peccs.2013.05.004.
- [9] Mette, B., Kerskes, H., Drück, H., Müller-Steinhagen, H. (2014). Experimental and numerical investigations on the water vapor adsorption isotherms and kinetics of binderless zeolite 13X. *International Journal of Heat and Mass Transfer*, vol. 71, p. 555-561, DOI:10.1016/j.ijheatmasstransfer.2013.12.061.
- [10] Banaei, A., Zanj, A. (2021). A review on the challenges of using Zeolite 13X as heat storage systems for the residential sector. *Energies*, vol. 14, no. 23, art. ID 8062, DOI:10.3390/en14238062.
- [11] Rogala, Z., Kolasinski, P., Gnutek, Z. (2017). Modelling and experimental analyzes on air-fluidised silica gel-water adsorption and desorption, *Applied Thermal Engineering*, vol. 127, p. 950-962, DOI:10.1016/j.applthermaleng.2017.07.122.
- [12] De Antonellis, S., Colombo, L.P.M., Castellazzi, P., Rossetti, A., Marocco, L. (2024). System integration analysis of a zeolite 13x thermal energy storage. *Energy and Built Environment*, vol. 5, no. 4, p. 568-579, DOI:10.1016/j.enbenv.2023.04.006.